FIND THE ROOT CAUSE OF WELDING-INDUCED DISTORTION BY NUMERICAL MODELING METHOD

by Chon L. Tsai[1]

[1] Department of Industrial, Welding and Systems Engineering, The Ohio State University
1248 Arthur E. Adams Drive, Columbus, Ohio 43221, USA, tsai.1@osu.edu

ABSTRACT

The cumulative, shrinkage plastic strains and their distributions in the weld joint after completion of the welding process determine welding-induced distortion. Although the weldment undergoes many complex physical and metallurgical changes during welding, only the material plastic temperature range and its cooling history below this temperature range influence the final state of the cumulative shrinkage plastic strains. In addition, for structural welds, these plastic strains are uniform, except in the arc start and stop regions, along the weld. Therefore, the plastic strain-based "inherent shrinkage model" is effective and accurate to describe welding-induced distortion. This paper presents the theoretical background and numerical verification of this root cause.

KEYWORDS

Welding distortion, cumulative plastic strains, inherent shrinkage strain, distortion prediction, material plastic temperature

INTRODUCTION

One common problem associated with welding, that has been realized and documented for many years, is the dimensional tolerance and stability of the finished products. In making a weld, the heating and cooling cycle always causes shrinkage in both base metal and weld metal, and the shrinkage forces tend to cause a degree of distortion. Machining of a welded product may cause dimensional changes of the product due to relaxation of weld residual stresses. As a result of welding, the finished product may not be able to perform its intended purpose due to poor fit-up, vibration problems, high reaction stresses, reduced buckling strength, premature cracking or unacceptable appearance. Control of weld distortion is a vital task in welding manufacturing.

Attempts to understand weld distortion using predictive methodology, parametric experiments, or empirical formulations have been made by many researchers since 1950th. Attempts have also been made in recent years to predict weld distortion through computer simulations of welding process using the finite element analysis (FEA) method. One significant conclusion from these studies leads to that the final weld distortion is not so much influenced by the weld heating cycle, but instead occurs due to shrinkage in the weld metal and its adjacent base metal during cooling when the yield strength and modulus of elasticity of the material restore to its higher values at lower temperatures. Therefore, analysis of the shrinkage phenomena of welds alone may be sufficiently accurate to predict the weld distortion. This conclusion has led to the development of a modeling scheme referred to as the "inherent shrinkage model" by some researchers. The root cause for welding-induced distortion may be described using a plasticity-based hypothesis.

THE HYPOTHESIS

In a welded joint, the expansion and contraction forces act on the weld metal and its adjacent base metal. As the weld metal solidifies and fuses with the base metal, it is in its maximum expanded state. However, at this point, the weld metal and its adjacent base metal are at high temperatures and have little strength or rigidity. The volume expansion causes local thickening in the weld area, but is incapable of causing significant amount of plastic strains in the cooler joint neighborhoods. On cooling, it attempts to contract to the volume it would normally occupy at the lower temperature, but it is restrained from doing so by the adjacent cooler base metal. Stresses develop within the weld, finally reaching the yield strength of the weld metal. At this point the weld stretches, or yields, and thins out, thus adjusting to the volume requirements of the lower temperature. But only those stresses that exceed the yield strength of the weld metal are relieved by this accommodation. By the time the weld reaches room temperature, the weld will contain locked-in tensile stresses (residual stresses) of yield magnitude and the base metal away from the weld is usually in compression with smaller magnitude. The internal tensile and compressive forces are in equilibrium with the joint deforming to comply with the strain compatibility. The residual stress distributions and the amount of weld distortion depend on the final state of the plastic strain distributions and their compatibility in the joint.

The welding-induced incompatible inelastic strains in the weldment during the heating and cooling weld cycles include transient thermal strains, cumulative plastic strains, and the final inherent shrinkage strains. At any instant during welding, the incompatible thermal strains resulting from the nonlinear temperature distributions

generate the mechanical strains, which lead to the incremental plastic strains in the weldment if yielding occurs. The incremental plastic strains accumulate over the periods of heating and cooling. Upon completion of the welding cycles, the cumulative plastic strains interact with the weldment stiffness and the joint rigidity resulting in the final state of residual stresses and distortion of the weldment. This final state of the inelastic strains, which are always compressive, is referred to as the "inherent shrinkage strains."

Welding-induced, incompatible plastic strains (assuming a 2-D plane-strain condition for illustration purpose) at each heating or cooling time increment may be described mathematically as follows:

$$\nabla^2(\sigma_x + \sigma_y) = -\frac{E}{1-\nu}\nabla^2(\alpha\theta) - [g(x,y) + \Delta g(x,y)] \quad [1]$$

where ∇^2 is the Laplacian operator, σ_x and σ_y are thermal stress components in the respective x and y directions, E is Young's modulus, ν is Poisson's ratio, α is thermal expansion coefficient, θ is a temperature function, g(x,y) is a cumulative plastic strain function, and $\Delta g(x,y)$ is the plastic strain increment function over each thermal loading step. The plastic strain functions may be written as follows:

$$g(x,y) = \frac{E}{1-\nu^2}\left(\frac{\partial^2\varepsilon_x^p}{\partial y^2} + \frac{\partial^2\varepsilon_y^p}{\partial x^2} - 2\frac{\partial^2\varepsilon_{xy}^p}{\partial x\partial y}\right) - \frac{\nu E}{1-\nu^2}\nabla^2(\varepsilon_x^p + \varepsilon_y^p) \quad [2]$$

$$\Delta g(x,y) = \frac{E}{1-\nu^2}\left(\frac{\partial^2(\Delta\varepsilon_x^p)}{\partial y^2} + \frac{\partial^2(\Delta\varepsilon_y^p)}{\partial x^2} - 2\frac{\partial^2(\Delta\varepsilon_{xy}^p)}{\partial x\partial y}\right) - \frac{\nu E}{1-\nu^2}\nabla^2(\Delta\varepsilon_x^p + \Delta\varepsilon_y^p) \quad [3]$$

The Laplacian thermal strains are governed by the rate of enthalpy change in the weldment. Upon completion of the heating and cooling cycles the cumulative plastic strains in the weldment are usually compressive and become the inherent shrinkage strains, $g^I(x,y)$, that interact with the structural rigidity to result in residual stresses (σ_x^R and σ_y^R) and distortion (ε_x^D and ε_y^D). Residual stresses may be written with a possible reverse yielding, $g^R(x,y)$ as follows:

$$\nabla^2(\sigma_x^R + \sigma_y^R) + g^R(x,y) = -g^I(x,y) \quad [4]$$

Distortion may be written in the form of final total strains as follows:

$$\varepsilon_x^D - \varepsilon_x^I = \frac{1}{E}\left[\sigma_x^R - \nu\left(\sigma_y^R + \sigma_z^R\right)\right] + \varepsilon_x^{PR} \quad [5]$$

$$\varepsilon_y^D - \varepsilon_y^I = \frac{1}{E}\left[\sigma_y^R - \nu\left(\sigma_z^R + \sigma_x^R\right)\right] + \varepsilon_y^{PR} \quad [6]$$

$$\varepsilon_z^D - (\varepsilon_x^I + \varepsilon_y^I) = \frac{1}{E}\left[\sigma_z^R - \nu\left(\sigma_x^R + \sigma_y^R\right)\right] - \varepsilon_x^{PR} - \varepsilon_y^{PR} = cons\tan t \quad [7]$$

$$\gamma_{xy}^D - \gamma_{xy}^I = \frac{2(1+\nu)}{E}\tau_{xy}^R + \gamma_{xy}^{PR} \quad [8]$$

where the superscripts: D represents distortion strains, I represents the inherent (cumulative) shrinkage strains, R represents residual stresses, and PR represents plastic strains due to reverse yielding.

With known distortion strains determined from the inherent shrinkage plastic strains, the distortion shape of a weldment can be determined by integrating these strains with respect to spatial coordinate variables. For a simple, longitudinal plate bending case (e.g. welding along one edge of a long plate), the total strain at the center of gravity of any cross-sections, ε_{cg}^D and its curvature, C, may be written as follows:

$$\varepsilon_{cg}^D = \frac{\iint_{A_I}\varepsilon_x^I dydz}{A_{section}} \quad [9]$$

$$C = \frac{Z_{cg}^{section} - Z_{cg}^I}{I}\iint_{A_I}\varepsilon_x^I dydz \quad [10]$$

where A_I is the shrinkage strain area that contains the inherent shrinkage plastic strains and $A_{section}$ is the geometric cross-sectional area. $Z_{cg}^{section}$ and Z_{cg}^{I} are distances from weld to the centers of gravity of these two areas, respectively.

For a inherent plastic strain distribution uniform along the welding direction, the maximum bending distortion,δ may be determined by integrating the curvature of all cross-sections along the weld length and can be written as

$$\delta = \frac{CL^2}{8} \qquad [11]$$

Equations 1 through 8 demonstrate that the cumulative plastic strains govern the final state of residual stresses and weldment distortion. Therefore, an engineering approach to estimating welding-induced residual stresses or distortion is to establish the relationships between these plastic strains and variables associated with welding process, joint design, and structural detail. Some physical phenomena occurs during welding may not be described using these theoretical equations, which effects can only be analyzed by the numerical simulations. During the heating process all the strains in the molten pool relax to the nil strain state. Upon solidification the weld metal shrinks from the melting temperature resulting in high shrinkage stresses. The inherent shrinkage strains should include these shrinkage strains. However, depending upon the relative stiffness of the shrinkage zone and the elastic-resistance zone in the base metal, only those inherent strains within twice of the yield magnitude are effective in causing the final state of residual stresses and distortion.

The inherent shrinkage strains are primarily caused by material softening and nonlinear thermal gradients in the cooler areas. The inherent shrinkage strains are uniform along the weld length, except in the areas of arc start and stop. They are nearly uniform within the softening area in the direction transverse to the weld. The strain magnitude decreases at a steep slop to zero within a short distance from the edges of the softening zone. The peak temperature attained in the weldment are uniquely related to the longitudinal inherent shrinkage strains due to relatively large stiffness ratio between he soften zone and its cooler surroundings. The peak temperature distribution can be used to estimate the longitudinal inherent shrinkage strains with good accuracy. The longitudinal residual stresses and the longitudinal cambering can therefore be determined from the peak temperature distributions. Buckling can also be predicted in large thin-plate weldments. The peak temperatures alone are insufficient to determine the transverse inherent shrinkage strains because of the smaller stiffness ratio and its sensitivity to the joint thickness and the external constraint conditions. Nevertheless, with a correction procedure considering the material incompressibility, the modified transverse inherent shrinkage strains can be used to estimate with good accuracy the transverse residual stresses and angular distortion of the weldment.

VERIFICATION BY NUMERICAL MODELING METHOD

To illustrate the theoretical basis of the inherent shrinkage behavior of weldment, a simple welding case that simulates a welding arc moving along one edge of a plate (ASTM A36 steel with matching electrode, 300mm x 50mm x 8mm) was modeled and analyzed. In this study, temperature-dependent thermal and mechanical properties of A36 steel were incorporated in the numerical analysis. Several physical phenomena associated with the welding process, including moving arc source, filler metal addition, and plastic strain relaxation due to melting, were modeled. Results analyzed from this modeling study included peak temperature, cumulative plastic strains, and total strains.

Assuming two ellipsoidal functions for arc heat distribution ahead and behind the arc, respectively, the heat input, calculated from products of arc efficiency, welding current, and arc voltage, was applied to the welding edge of the plate. The heat distribution was uniform through the plate thickness. Assuming that the heat intensity along the boundary of the ellipsoids equals to 5% of the maximum value at the arc center, the generic ellipsoidal heat function may be written as follows:

$$\dot{q}(x,y) = \frac{6 f \eta V I}{5.76 \pi H \beta} Exp\left(\frac{-3(x-St)^2}{5.76\beta^2} + \frac{-3y^2}{5.76} \right) \qquad [12]$$

where $\dot{q}(x,y,t)$ is power density (W/mm^3); t is time elapsed after arc initiation (second); x, y are global coordinate axes with origin at the arc initiation center (x is along weld axis and y is in the direction transverse to weld) (mm); H is plate thickness (mm); I is average welding current (A); S is arc travel speed (mm/s); V is arc voltage (volt); f is weight factor (1.4 behind the arc and 0.6 ahead the arc); η is arc efficiency (0.55); β is the lag factor that determines the slop of the heat distribution function in x-direction (4.0 behind the arc and 1.0 ahead the arc). The 5.7 factor is a square of the semi-axes of the ellipsoidal boundaries. The weight and lag factors were calibrated with published experimental

data[1]. A similar approach dubbed as "double ellipsoidal heat source model" was introduced by Goldak et. al.[2,3] in 1984 and 1986.

Figure 1 shows the predicted temperature contours surrounding the welding arc at 28.57 seconds after arc initiation (603 cal/cm; 160 A, 20 volts, 7 mm/s, and 0.55 arc efficiency). The arc location at this instant is 200 mm from the edge where arc initiates. Since the material softens as the temperature increases beyond its plastic temperature range, plastic strains build up quickly and are usually in compression. These plastic strains are relaxed when melting occurs. Therefore, the thermal parameter that governs the cumulative plastic strains is the peak temperature the material can reach during welding. Although plastic strains may also be formed due to large incompatible thermal strains, the softening effect is usually so large that overrides the incompatible thermal strain effect. The peak temperatures may well define the shrinkage plastic zones. Figure 2 shows that the peak temperatures are independent of weld axis, except in the regions of arc start and stop. This illustrates that, for structural welding, simultaneously laying weld bead along the entire joint that reaches the same peak temperature condition as predicted from the moving source model would result in similar state of plastic strains.

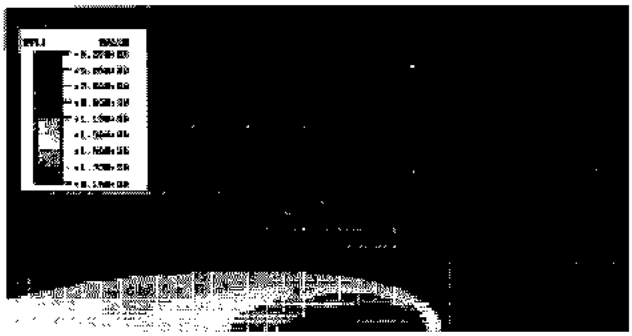

Fig. 1 Quasi-steady temperature contours

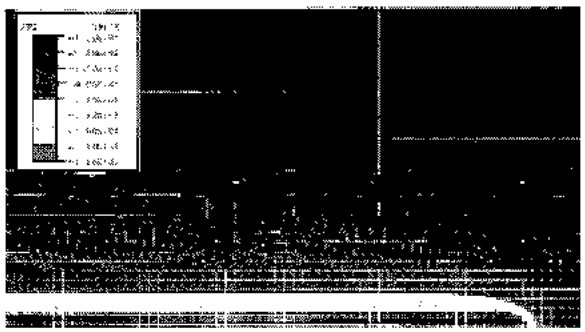

Fig. 2 Peak temperature contours

Figure 3 shows the contours of the cumulative plastic strain components that are parallel and transverse to weld, respectively. Both plastic strain components are uniform along the weld, except at the ends. The longitudinal elastic strains are in tension in the weld layer (1-mm depth) due to shrinkage from a strain-free state (i.e. strain relaxation). They become compressive outside the weld zone. The depth of this plastic zone is about 15 mm. This plastic strain component governs the bending distortion of the plate. The transverse plastic strains are compressive within the weld layer (1 mm) and tensile outside the weld. The zone depth of the transverse plastic stains is larger than 20 mm. The magnitude of the transverse plastic strains, which is greater than their longitudinal counterpart, results in transverse shrinkage in the plate. The longitudinal plastic strains cause bending curvature.

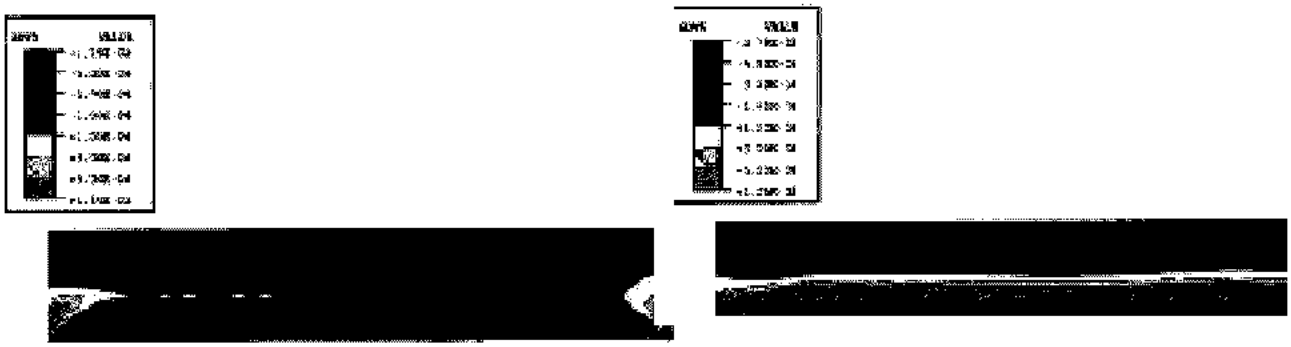

Fig. 3 Plastic strain contours (left: longitudinal and right: transverse)

Figure 4 (left) shows the temperature distributions in eight cross-sections with respect to an arc location. Positive sign indicates the cross-section ahead the arc and negative sign indicates the cross-sections behind the arc. A quasi-steady state heating and cooling process in the plate is shown. Figure 4 (right) shows a plot of peak temperature distribution in ten cross-sections. Because of its uniformity in the longitudinal direction, a single curve is shown in all

cross-sections. This curve also represents the maximum temperature boundary of all temperature curves experienced during the heating and cooling cycles. Figure 4b shows a melt penetration depth, which is a little larger than the weld layer. This melt zone goes through the strain relaxation process during welding. The plastic temperature range shows other zones that go through either partial or full softening process. The cumulative plastic strains that govern the state of residual stresses and distortion are contained primarily in these zones bounded by the melt penetration depth and the lower softening temperature.

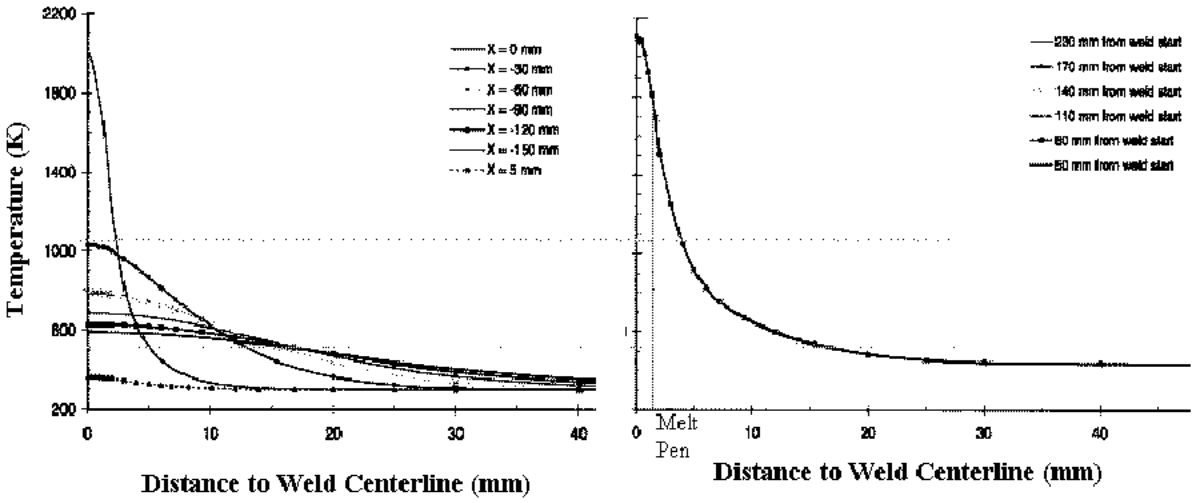

Fig. 4 Temperature distributions at 8 cross-sections (left: heating /cooling cycles and right: peak temperature contours)

Figure 5 plots two longitudinal strain distributions in the same figure, cumulative plastic strain and total strain. High tensile plastic strain is shown inside the melt penetration zone and compressive plastic strain is shown outside the melt penetration zone but within approximately a 15-mm depth. The tensile plastic strain in the melt penetration zone may be regarded as a product from reverse yielding, since this zone shrinks from a free-strain state. The longitudinal residual stress is also in tension with yield magnitude. The compressive plastic strain is caused primarily due to suppression of thermal strains by the cooler surrounding materials during the heating cycle. The depth of this compressive plastic strain zone coincides with the boundary of the softening temperature (approximately 15 mm). In Fig. 5, a linear distribution of total strain is obvious, except in the weld region. The nonlinear deformation of the cross-section in the weld and its surrounding area is due to softening effect during the heating cycle. With the weld temperature returning to its initial (room) condition, the difference between total strain and plastic strain represents the mechanical strain that results in residual stress. The only caution in regard with this assessment is that, in the melt penetration zone, residual stress is in tension of yield magnitude due to weld shrinkage.

As shown by the plastic and total strain curves in Fig. 5, welding-induced distortion is caused by a combination of weld (including penetration) shrinkage and the cumulative plastic strains. The black dot line shows linear total strain approximation. To develop an engineering approach to distortion prediction, a simple "Strength of Materials" type of analysis may be usefully defined as an equivalent mechanical system that incorporates all shrinkage mechanisms using the concept of "inherent shrinkage strain". Figure 6 shows the inherent shrinkage strain derived from Fig. 5. The total strain at the center of gravity (Equation 9) of any cross-section is the ratio of the inherent shrinkage strain area to the geometric cross-section area. The distortion curvature (Equation 10) of the cross-section is a product of distance that is between centers of gravity of the geometric cross-section and the inherent shrinkage strain area, and the ratio of the inherent shrinkage strain area to the moment of inertia of the geometric cross-section. This inherent shrinkage strain area must be equivalent to the combined areas of cumulative shrinkage plastic strain and weld shrinkage strain.

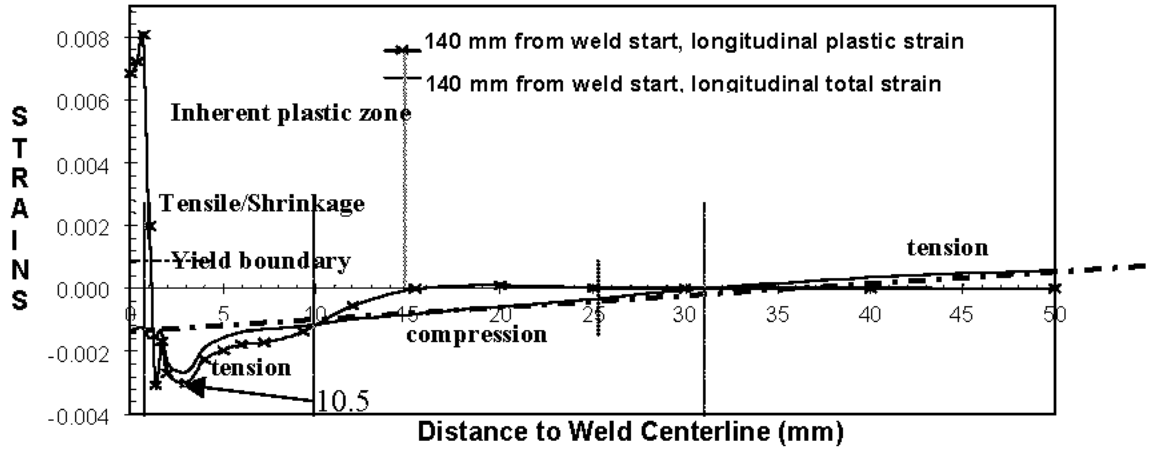

Fig. 5 Mechanical strains showing total and cumulative plastic strains

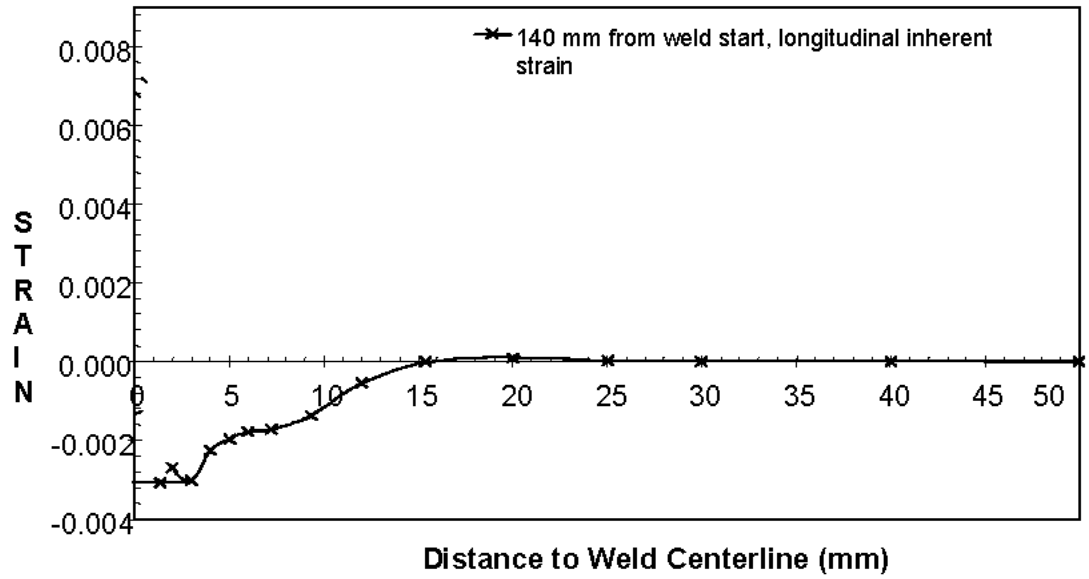

Fig. 6 Inherent shrinkage strains in accordance with the cumulative plastic strains as shown in Fig. 5

As shown in Equations 8 and 9 the total strain and the curvature are functions of the geometrical properties of the two areas. The geometric cross-section area is a defined parameter. The inherent shrinkage strain area can be determined from the cumulative plastic strains. Due to the fact that this plastic strain doesn't vary along the weld direction, the inherent shrinkage strain may be introduced into the weld joint by defining a shrinkage volume along the joint that produces an equivalent plastic strain area and location of its center of gravity. The inherent shrinkage strain can be introduced into a mechanical analysis system by describing an initial temperature to the weld and let it cool back to the initial temperature of the joint. This technique is dubbed as "Thermal Shrinkage Model". Or, springs with equivalent shrinkage rigidity may be placed along the joint to obtain the inherent shrinkage strain[4].

COMPARISON WITH OKERBLOM'S DATA[5]

Okerblom publishes a book in 1955, which included experimental distortion data of welding along the edge of a plate. A parametric study on welding heat input and travel speed using the numerical model described in this paper was conducted to provide a basis for discussing the validity of the numerical results by comparing them with the experimental data (Figure 7). For a constant travel speed of 7 mm/s, the cross-section curvature increases with the linear heat input that is normalized by the geometric cross-sectional area (i.e. equivalent energy density). For a given energy density of 150 cal/cm^3, the cross-section curvature would increase with travel speed. The experimental curve shows that the curvature increases with the energy density, reaches a plateau, and decreases after this plateau. A

rational explanation for this trend is as follows: (1) within the low energy density range, increasing energy density would increase the penetration depth of the melt zone and the size of the cumulative plastic strain zone, which results in greater curvature, and (2) within the high energy density range, increasing energy density would also increase the melt penetration depth and the size of the cumulative plastic strain zone, however, the centers of both zones move closer to the center of the geometric cross-section, which reduces the bending moment arm and the resulting curvature.

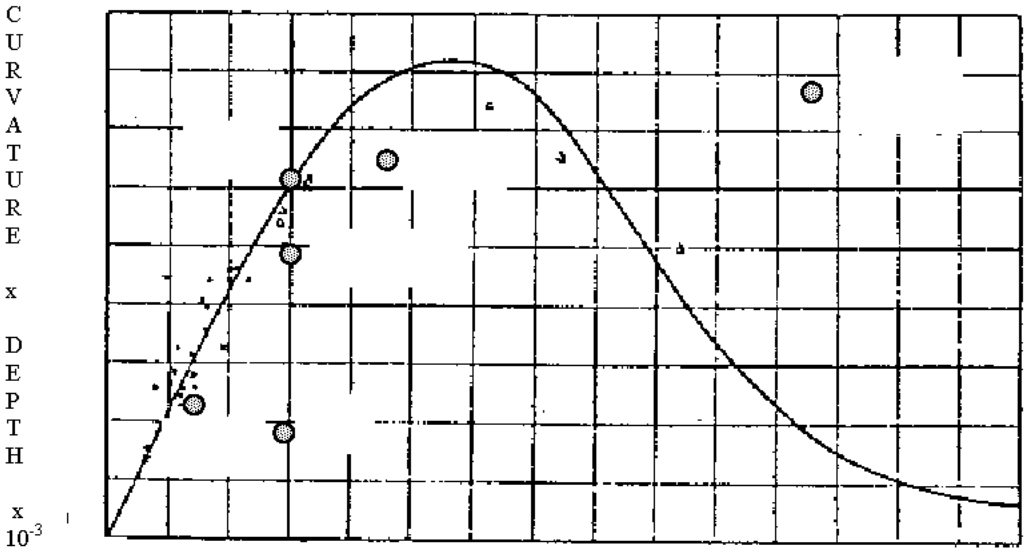

$$\frac{0.24 \bullet Efficiency \bullet Amp \bullet Volt}{Travel.Speed \bullet Area}$$

Fig. 7 Numerical results vs. experimental data by Okerblom[5]

CONCLUDING REMARKS

Although the inherent shrinkage model has been demonstrated to be accurate, convenient, and cost effective in the prediction of structural weld distortion, several fundamental issues remain unsolved. The inherent shrinkage model will need calibration constants for different applications. These calibration constants will depend on the thermal characteristics of the welding process and the geometric details of the joint. For example, the submerged arc welding process will result in very distinct thermal characteristics in the weldment from that caused by the shielded metal arc welding process. Welding of thick joints will result in complete different calibration constants than welding of thin sheet metals. To prescribe the initial shrinkage temperature in the joint, weld nugget area, which can be a well defined area, is usually used as the volume of domain for the prescribed temperatures. For the conduction shrinkage model, the metal shrinkage in the base material is controlled by the thermal diffusion process and the temperature-dependent mechanical properties, as well as the thermal affected areas by heat conduction from the prescribed enthalpy state in the weld. For the weld shrinkage model, no base metal shrinkage is considered.

REFERENCES

1. Feng, Z. L., Cheng, W. T., and Chen Y. S., "Development of New Modeling Procedures for 3D Welding Residual Stress and Distortion Assessment," EWI CRP Report SR9818, November 1998
2. Argyris, J. H., Szimmat, J. and William, K. J., "Computational Aspects of Welding Stress Analysis," Computer Methods in Applied Mechanics and Engineering, Vol. 33, 1982, pp. 635-666
3. Goldak, J., Bibby, M., Moore, J., House, R., and Patel, B., "Computer Modeling of Heat Flow in Welds Model for Welding Heat Source," Metallurgical Transactions B, 17B, 1986, pp. 587-600
4. Tsai, C. L. and Shim, Y. L., "Determination of Welding-Induced Shrinkage Strains for Distortion Prediction of Welded Frame Structures," Research Report submitted to General Motors Technical Center, June 1993
5. Okerblom, H. O., "the Calculations of Deformations of Welded Metal Structures," MASHGIZ, Moscow, 1955